ORNL/TM-11520

ornl

OAK RIDGE NATIONAL LABORATORY

MARTIN MARIETTA

Power and Particle Balance Studies Using an Instrumented Limiter System on ATF

T. Uckan
P. K. Mioduszewski
T. S. Bigelow
J. C. Glowienka
S. Hiroe
M. Murakami
J. B. Wilgen
W. R. Wing

MANAGED BY
MARTIN MARIETTA ENERGY SYSTEMS, INC.
FOR THE UNITED STATES
DEPARTMENT OF ENERGY

ORNL/TM-11520
Dist. Category UC-426

Fusion Energy Division

POWER AND PARTICLE BALANCE STUDIES USING AN INSTRUMENTED LIMITER SYSTEM ON ATF

T. Uckan
P. K. Mioduszewski
T. S. Bigelow
J. C. Glowienka
S. Hiroe
M. Murakami
J. B. Wilgen
W. R. Wing

Date Published: June 1991

Prepared for the
Office of Fusion Energy
Budget Activity No. AT 10

Prepared by the
OAK RIDGE NATIONAL LABORATORY
Oak Ridge, Tennessee 37831-6285
operated by
MARTIN MARIETTA ENERGY SYSTEMS, INC.
for the
U.S. DEPARTMENT OF ENERGY
under contract DE-AC05-84OR21400

CONTENTS

ABSTRACT

Power and particle balance studies on the Advanced Toroidal Facility (ATF) torsatron are carried out using a rail limiter system. Both top and bottom limiters are made of graphite tile arrays, and these tiles are instrumented with thermocouples and Langmuir probes for calorimetric and particle flux measurements. Initial experimental results indicate that the limiter power loss accounts for about 12% of the total and the radiation loss for about 30% of the total; the rest of the plasma heating power appears to be going to the vessel wall. The particle flux to the limiters is also about 18%. The fractions of power and particle flux to the limiters are relatively lower than in tokamaks because of the low edge safety factor, $q \sim 1$ rather than $q \sim 3$ as in a typical tokamak, at the natural boundary of the ATF plasma (which results from the magnetic stellarator configuration of this currentless device). Therefore, for limiters of the same size, these fractions are about a factor of q lower in ATF than in a comparable tokamak device.

1. INTRODUCTION

The instrumented limiter system (UCKAN *et al.*, 1988a) in the Advanced Toroidal Facility (ATF) torsatron (LYON *et al.*, 1986) is designed to study the characteristics of the scrape-off layer (SOL), that is, the profiles of the energy and particle fluxes in the plasma edge region. The stellarator configuration of the ATF has a poloidal multipolarity $l = 2$, 12 field periods ($M = 12$), a major radius $R_0 = 2.1$ m, and an average plasma radius $\bar{a} = 0.27$ m. The externally produced currentless magnetic configuration has moderate shear; that is, the central rotational transform ($\iota/2\pi = 1/q$) of 0.3 becomes 1.0 at the last closed flux surface (LCFS). The poloidal cross section of the plasma varies with the toroidal angle ϕ. At the locations of the limiters, $\phi = 0°$ and 30°, the plasma cross section is vertically elongated; at $\phi = 15°$, it is horizontally elongated. The physical dimensions of the limiters in ATF are shown in Fig. 1, and the details of their design are given by HAHS *et al.* (1987). The system consists of two movable rail limiters, one located at the top of the vacuum vessel and one at the bottom, separated toroidally by one field period (30°). Each limiter module has 11 individual graphite tiles, mounted on a water-cooled stainless steel base plate. The tiles form calorimetric arrays for measuring the energy deposition profile and the total deposited energy for the power balance studies. The front faces of the limiters are shaped for constant heat flux in the toroidal direction to handle 3 MW of power during a 0.3-s heating pulse without reaching a surface temperature of 1500°C. The central tile incorporates a gas puff nozzle and Langmuir probes for particle flux measurements along the field line in the SOL that provide information on the particle balance. Figure 1 shows the configuration of the top limiter on ATF when it is located at the LCFS and also shows the center tile and its surface shape (MIODUSZEWSKI *et al.*, 1989).

In Section 2, the equations of interest for calculating the power and the particle balance from the measurements of the instrumented limiter are discussed. In Section 3, the formalisms developed are applied to the ATF plasma. Brief discussions follow in Section 4.

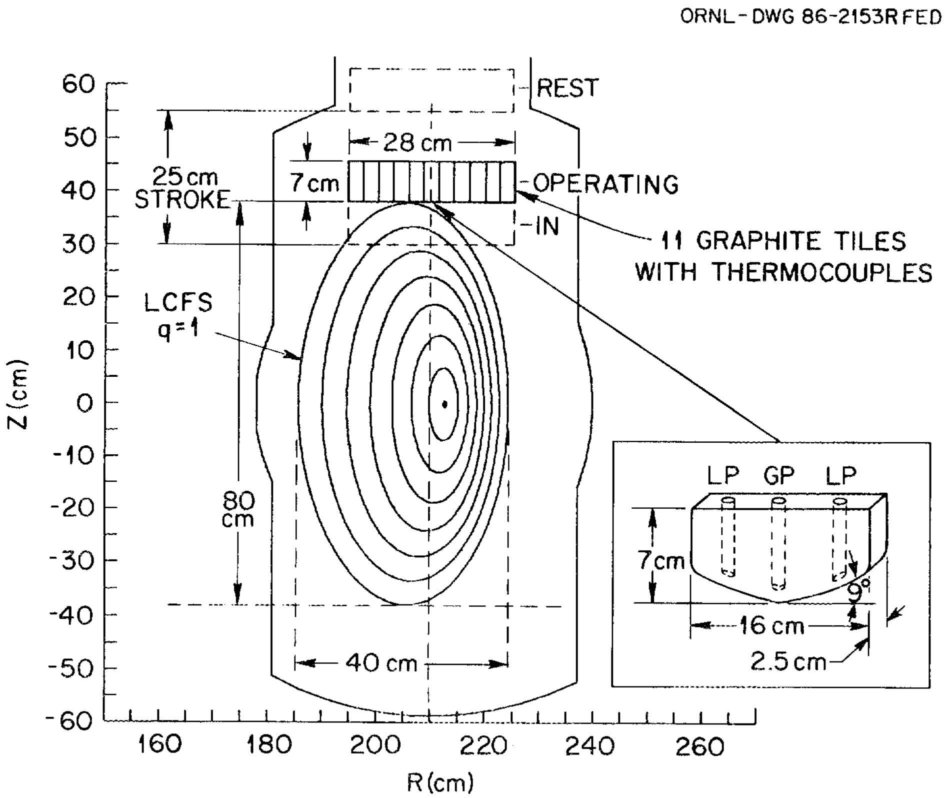

FIG. 1. Location of the top rail limiter in ATF. The inset shows the central tile with Langmuir probes and the tile surface shape.

2. EQUATIONS OF INTEREST

When the limiters are placed at the LCFS, as shown in Fig. 2, each receives a fraction ε_p of the power P_{out} that leaves the core plasma and a fraction ε_F of the total particle efflux Φ_{out}. The power coverage of each limiter is defined as

$$\varepsilon_p = P_{Lim}/P_{out} \,, \tag{1}$$

and the particle flux coverage of each limiter is

$$\varepsilon_F = \Phi_{Lim}/\Phi_{out} \,, \tag{2}$$

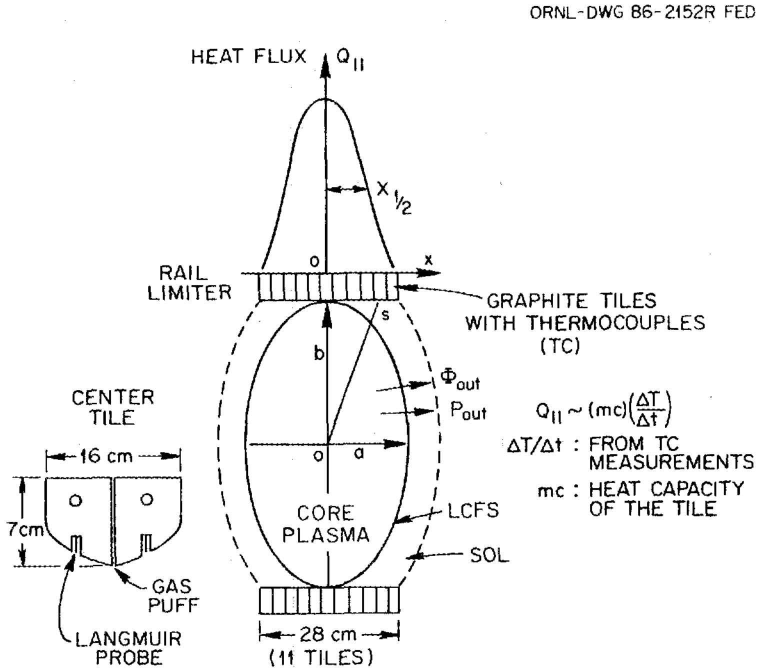

FIG. 2. Schematic of the LCFS, where the limiters are located, and the expected heat deposition profile on the rail limiter. The top and the bottom limiters are separated 30° toroidally. The ATF LCFS parameters are a = 0.2 m and b = 0.4 m, and the average plasma radius $\bar{a}$ = 0.27 m. Here P_{out} and Φ_{out} are the total power and the particle efflux leaving the core plasma, respectively. In the SOL, the heat flux $Q_{||}$ and the particle flux $\Gamma_{||}$ along the field lines are decaying exponentially.

where P_{Lim} and Φ_{Lim} are the power and the total particle flux received by each limiter, respectively. From the total input plasma heating power P_{input} and the radiated power P_{rad} estimated from bolometric measurements (HIROE *et al.*, 1990), the power that leaves the core plasma by conduction and convection is $P_{out} = P_{input} - P_{rad}$. The total particle efflux from the core plasma, whose total number of electrons is $N = \langle n \rangle V_p$ with an average particle confinement time of τ_p, is $\Phi_{out} = N/\tau_p$, where $\langle n \rangle$ is the volume-averaged electron density and V_p is the core plasma volume.

In the SOL, the heat flux $Q_{||}$ and the particle flux $\Gamma_{||}$ along the field lines are observed (MIODUSZEWSKI *et al.*, 1987; UCKAN *et al.*, 1988b) to decay exponentially with scale lengths of λ_q and λ_Γ, respectively. Given this observation, we can calculate P_{Lim} and Φ_{Lim} as follows. First, it is assumed that the LCFS of ATF, which is an island-free magnetic field configuration (COLCHIN *et al.*, 1990) as shown in Fig. 1, may be represented in terms of an ellipse whose small and large minor radii are a = 0.2 m and b = 0.4 m, respectively. On the limiter, tile j, which is located horizontally at a distance x_j from the center tile, is a distance s_j away from the LCFS. That is,

$$s_j = \sqrt{\left(x_j^2 + b^2\right)/\left(x_j^2 + a^2\right)}\left[\sqrt{\left(x_j^2 + a^2\right)} - a\right]. \tag{3}$$

The heat flux distribution across the limiter surface is $Q_{||}(x_j) = Q_0 \exp(-s_j/\lambda_q)$, with $Q_0 \equiv Q_{||}(s_j = 0)$ the heat flux at the LCFS. Therefore, the energy deposition profile on the limiter during a plasma discharge of duration Δt is $\Delta E_j \equiv \Delta E(x_j) = \Delta E(0)\exp(-s_j/\lambda_q)$, where $\Delta E(0) \equiv \Delta E(x_j = 0)$ is the energy increase at the limiter center tile, $x_j = 0$. Experimentally, the ΔE_j tile energy distribution is obtained from conventional calorimetric measurements and the heat capacity of the tiles. The e-folding characteristic scale length of the heat flux can be estimated from the half-width at half-maximum x_{HWHM} of the ΔE_j profile as $\lambda_q = -s(x_{\mathrm{HWHM}})/\ln 0.5$. Then the power received by each limiter is simply calculated from the summation of $\Delta E_j/\Delta t$ over the number of tiles of the limiter:

$$P_{\mathrm{Lim}} = \sum_{j=1,11} \Phi_0 P_0 \exp\left(-s_j/\lambda_q\right) \equiv f_p P_0 \quad ,$$

$$= f_p \left[2Q_0 w \int_0^\infty ds \exp(-s/\lambda_q)\right] = 2 f_p Q_0 w \lambda_q \, , \tag{4}$$

where $P_0 = \Delta E(0)/\Delta t$ is the power received by the center tile, which has a poloidal width w as shown in Fig. 3. Clearly, the technique described here provides no time resolution of the power flux during the plasma discharge, but it gives fairly accurate measurements of the power deposition profile on the limiters (MIODUSZEWSKI *et al.*, 1987).

The total particle flux over each limiter is obtained similarly by making use of $\Gamma_{||}(x_j) = \Gamma_0 \exp(-s_j/\lambda_\Gamma)$:

$$\Phi_{\mathrm{Lim}} = \sum_{j=1,11} \Phi_0 \exp\left(-s_j/\lambda_\Gamma\right) \equiv f_F \Phi_0 \quad , \tag{5}$$

ORNL-DWG 90M-2560 FED

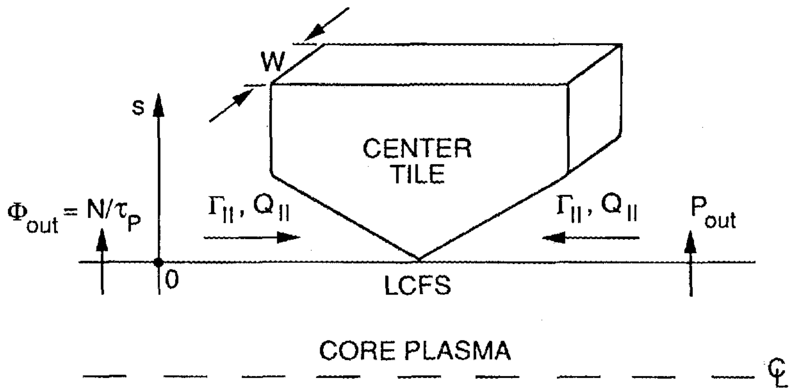

FIG. 3. Schematic of the limiter center tile on the LCFS and the SOL heat and particle fluxes.

with

$$\Phi_0 = 2\Gamma_0 w \int_0^{\infty} ds \exp(-s/\lambda_\Gamma) = 2\Gamma_0 w \lambda_\Gamma , \tag{6}$$

where $\Gamma_0 \equiv \Gamma_{||}(s_j = 0)$ is the particle flux at the LCFS and Φ_0 is the total particle flux received by the center tile. Experimentally, the Langmuir probe in the center tile gives Γ_0 from the measurements of the ion saturation current.

The parameters f_P and f_F defined here can be viewed as the shape factors of the limiter distribution for the power and the total particle flux, which are normalized to their values at the center tile. Figure 4 shows the dependence of these factors on their respective scale lengths λ. Moreover, with Eqs. (1), (2), (4), and (5), f_P and f_F can also be related to the power and the flux coverages of the limiter,

$$\varepsilon_P/\varepsilon_F = f_P/f_F . \tag{7}$$

This relationship is obtained from the power and particle balance relationships (UCKAN *et al.*, 1988b) at the edge:

$$P_o/Q_0 = P_{out}/\Phi_{out} = \gamma T_e(\lambda_q/\lambda_\Gamma) , \tag{8}$$

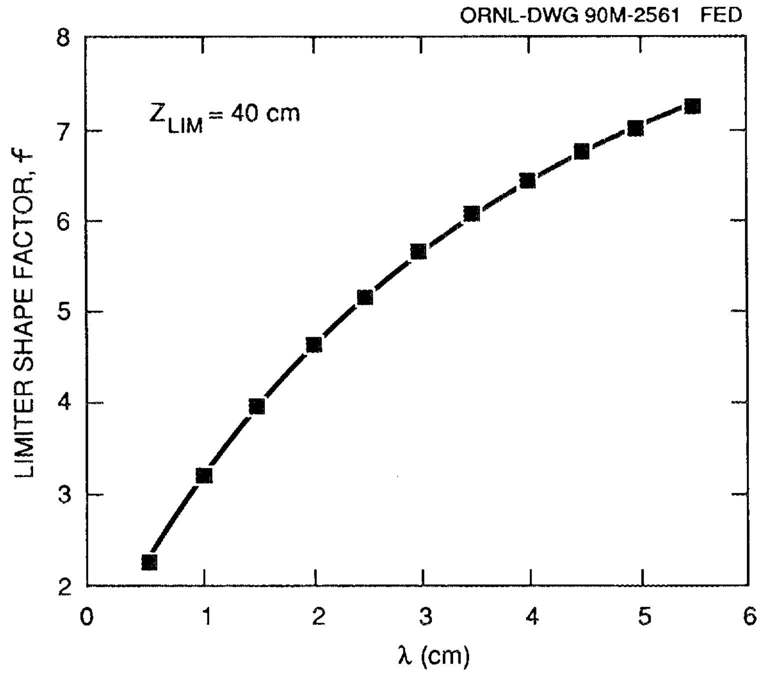

FIG. 4. Variations of the shape factors of the limiter distribution for the power f_p and particle flux f_F with their respective characteristic scale lengths λ.

where T_e is the electron temperature of the SOL plasma and γ is the heat transfer coefficient (STANGEBY, 1986), which is related to T_e, the ion temperature T_i, the species mass ratio $\mu = m_e/m_i$, and the secondary electron emission coefficient γ_s:

$$\gamma = 2T_i/T_e + 2/(1-\gamma_s) - 0.5\ \ln[2\pi\mu(1+T_i/T_e)/(1-\gamma_s)^2]\ , \tag{9}$$

and $\gamma \sim 15$ for a hydrogen plasma with $T_i/T_e \sim 1$, with $\gamma_s \sim 0.8$ for electrons with $T_e \sim 50$ eV incident to the carbon tiles (THOMAS, 1984).

It is useful to express the limiter flux coverage ε_F defined by Eq. (2) in terms of the limiter parameters. The total particle efflux in Eq. (2) is $\Phi_{out} = N/\tau_p = S_\perp \Gamma_\perp$, where $S_\perp = 4\pi \bar{a} R_0$ is the area of the LCFS in terms of $\bar{a}$ and R_0 and $\Gamma_\perp$ is the outward particle flux, which is perpendicular to the LCFS at radius $\bar{a}$. Furthermore, by again invoking the particle balance (UCKAN *et al.*, 1988b) at the LCFS, we can find

$$\varepsilon_F = qL_\theta(\text{eff})/2\pi\bar{a}, \tag{10}$$

where q is the safety factor at the LCFS and L_θ(eff) is the effective poloidal length of the limiter, which is obtained by noting that $\Phi_{Lim}/\Phi_o = f_F = L_\theta(\text{eff})/w$, or simply

$$L_\theta(\text{eff}) = w f_F \,. \tag{11}$$

The total particle efflux can be also estimated by combining the limiter calorimetric measurements for the power deposition and the center tile Langmuir probe measurements for the particle flux. Namely, from Eqs. (2), (5), and (7), it is found that

$$\Phi_{out} = (f_p/\varepsilon_p)\Phi_o \,. \tag{12}$$

Here Φ_o is obtained from Eq. (6) by using Γ_o from the limiter Langmuir probe measurements.

In Section 3 the formalisms discussed here are applied to a typical ATF plasma. The limiter power, the particle flux coverage, the global particle confinement time, and the power and particle balance are presented, and the experimental observations of these parameters are compared with these model calculations.

3. ATF RESULTS

The parameters of a typical 2-T electron cyclotron heated (ECH) plasma discharge in ATF with input power P_{input} = 300 kW are displayed in Fig. 5. The figure shows P_{input} from the two 53-GHz gyrotron heating sources, the line-averaged core plasma electron density $\bar{n}$, the plasma stored energy W_p, and the radiation power P_{rad}. The limiters, when they were at the vertical position z_{Lim} = 0.4 m, at the LCFS where q = 1, received P_{Lim} = 18 kW each during a Δt = 0.4 s discharge, as shown in Fig. 6. By using P_{rad} ~ 70–80 kW in Eq. (1), we find the power coverage of each limiter ε_p = 8% for P_{out} = 220 kW. From the limiter energy deposition profile, Fig. 7, x_{HWHM} = 6 cm; with this value in Eq. (3) the heat flux scale length becomes λ_q = 2.5 cm. Experimental observations from other edge Langmuir probe measurements (UCKAN *et al.,* 1989)

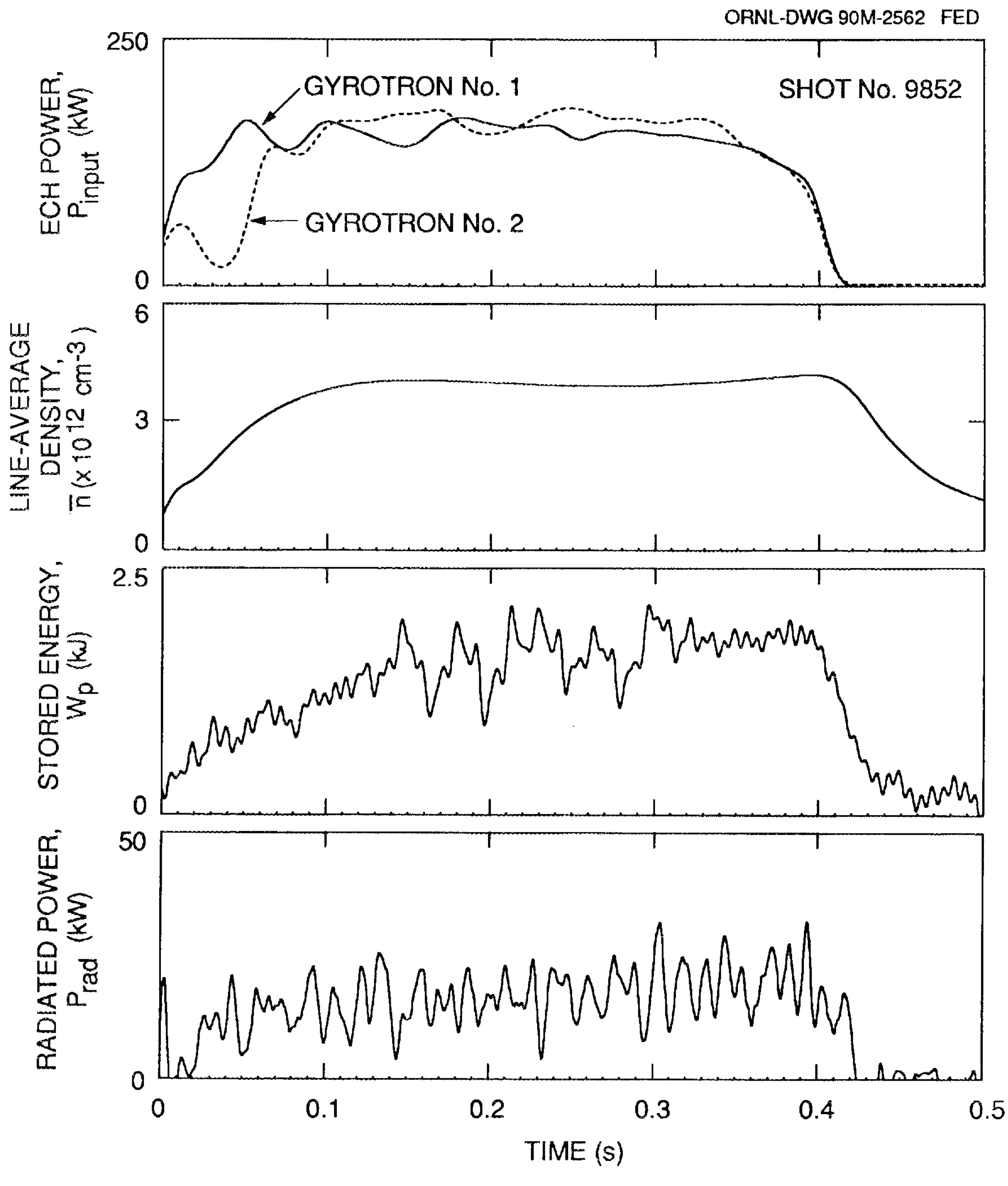

FIG. 5. Typical 2-T ECH plasma discharge parameters for ATF, showing time variations of the input heating power P_{input}, line-averaged plasma density $\bar{n}$, the stored energy W_p, and the radiation power P_{rad}.

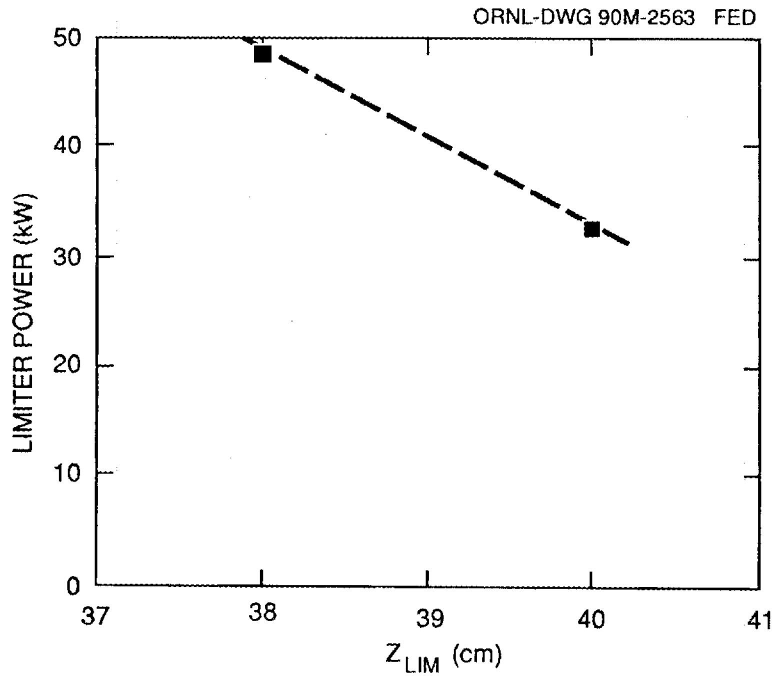

FIG. 6. The total limiter power deposition when the limiters are located at the LCFS, z_{Lim} = 40 cm, and 2 cm inside the LCFS.

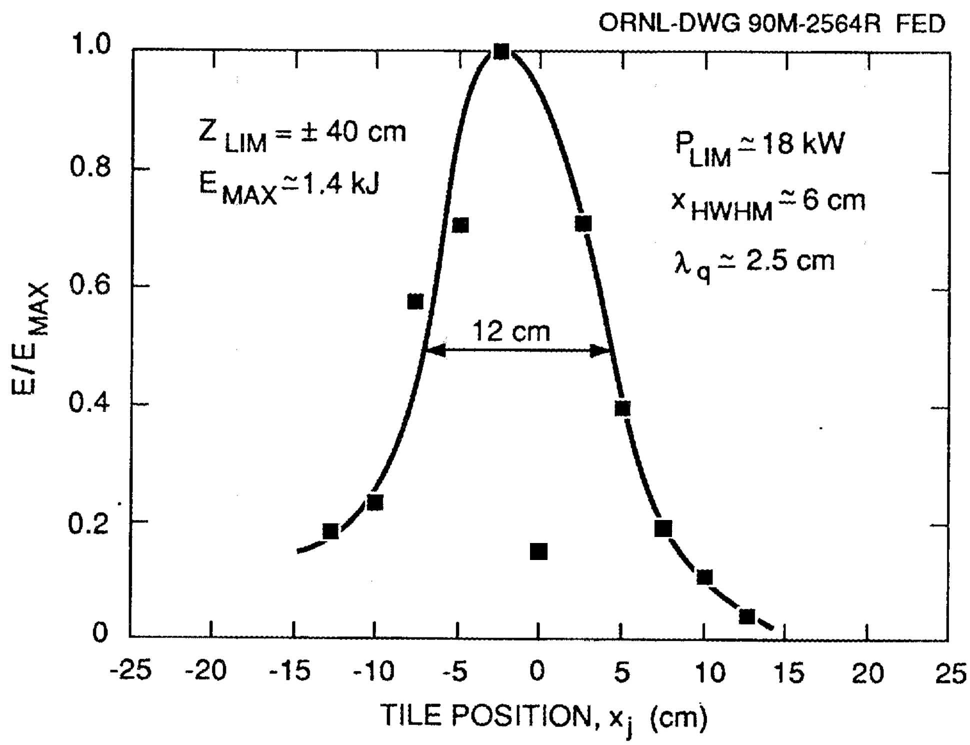

FIG. 7. The limiter energy deposition profile at the LCFS. x_{HWHM} = 6 cm, and the estimated λ_q = 2.5 cm.

indicate that the temperature e-folding characteristic scale length is much larger than the density scale length, by as much as a factor of 2. Therefore the flux scale length can be estimated (UCKAN *et al.*, 1988b) as $\lambda_\Gamma = 1.4 \times \lambda_q = 3.5$ cm. Using these values in Fig. 4 to get the limiter shape factors for power and flux, we find that $f_p = 5$ and $f_F = 6$. Then the particle flux coverage of the each limiter is calculated from Eq. (7):

$$\varepsilon_F = \varepsilon_p/(f_p/f_F) = 9.5\% \ .$$

This coverage may also be obtained from the calculation of the equivalent poloidal width of the limiter, Eq. (11). The poloidal width of the limiter tile $w = 2.54$ cm; thus,

$$L_\theta(\text{eff}) = wf_F = 2.54 \times 6 = 15.5 \text{ cm},$$

and in turn from Eq. (10) it is found that

$$\varepsilon_F(\text{calculation}) = 9\% \ ,$$

consistent with the earlier estimated value from the power coverage.

The particle efflux is estimated from Eq. (8); that is,

$$\Phi_{out} = P_{out}/\gamma T_e(\lambda_q/\lambda_\Gamma) = 220 \text{ kW}/(15 \times 50 \times 0.7) = 2.5 \times 10^{21} \text{ s}^{-1}.$$

Here $T_e = 50$ eV from the limiter Langmuir probe measurements is used for the SOL electron temperature. Using the core plasma volume $V_p = 3$ m^3 with the line-averaged density $\bar{n} = 5.5 \times 10^{12}$ cm^{-3} gives the total core plasma electrons $N = 1.7 \times 10^{19}$, which is obtained by taking $\langle n \rangle \sim \bar{n}$ since the ATF electron density profiles are observed to be almost flat. Hence the global particle confinement time is about

$$\tau_p = N/\Phi_{out} = 7 \text{ ms} \ .$$

This is comparable to the global energy replacement time, since the stored energy of the plasma is about $W_p = 1.9$ kJ for this discharge; thus,

$$\tau_e = W_p/P_{input} = 1.9\ \text{kJ}/300\ \text{kW} = 6.5\ \text{ms}\ .$$

The total particle efflux can also be estimated from Eq. (12). Taking the particle flux from the Langmuir probe measurements, $\Gamma_o = 6.5 \times 10^{18}\ \text{cm}^{-2}\cdot\text{s}^{-1}$, and using it in Eq. (6) gives $\Phi_o = 4.5 \times 10^{19}\ \text{s}^{-1}$ and, in turn, $\Phi_{out} = 2.8 \times 10^{21}\ \text{s}^{-1}$. This estimate is consistent with the value obtained from Eq. (8), and this result may further suggest that the value used for the heat transmission coefficient is a reasonable one based on the assumptions made in Eq. (9).

To see clearly the effects of the limiters on the flux coverage with respect to each other on ATF, we assume, for simplicity, a cylindrical geometry in poloidal angle (θ) and toroidal angle space for the LCFS. The top and bottom limiters of ATF are displayed in this configuration in Fig. 8. The limiter has a poloidal extent $\theta_L = L_\theta(\text{eff})/\bar{a} = 32°$ and a toroidal extent $\phi_L = L_\phi/R_o = 4°$, since $L_\theta(\text{eff}) = 15.5$ cm and $L_\phi = 16$ cm. Each limiter defines a flux tube through which the SOL particles flow and become available for deposition on the limiters. Clearly, these two limiters do not shadow each other (Fig. 8), so the total limiter flux coverage is about $\varepsilon_F(\text{total}) = 2 \times \varepsilon_F = 18\%$ of the total particle efflux. Similarly, the total power coverage of the limiters is about $\varepsilon_p(\text{total}) = 2 \times \varepsilon_p = 16\%$.

4. DISCUSSIONS

From the initial experimental results presented here, the power accountability of ECH plasmas in ATF is as follows. The radiation loss estimated from the bolometric measurements $P_{rad}/P_{input} \sim 30\%$, the limiter power loss $P_{Lim}(\text{total})/P_{input} \sim 12\%$, and the rest of the plasma heating power, about 58%, appears to be going to the vessel wall. The total limiter power coverage is about 16%, and the total limiter particle flux coverage is also about 18%. These fractions are relatively lower than those in tokamaks

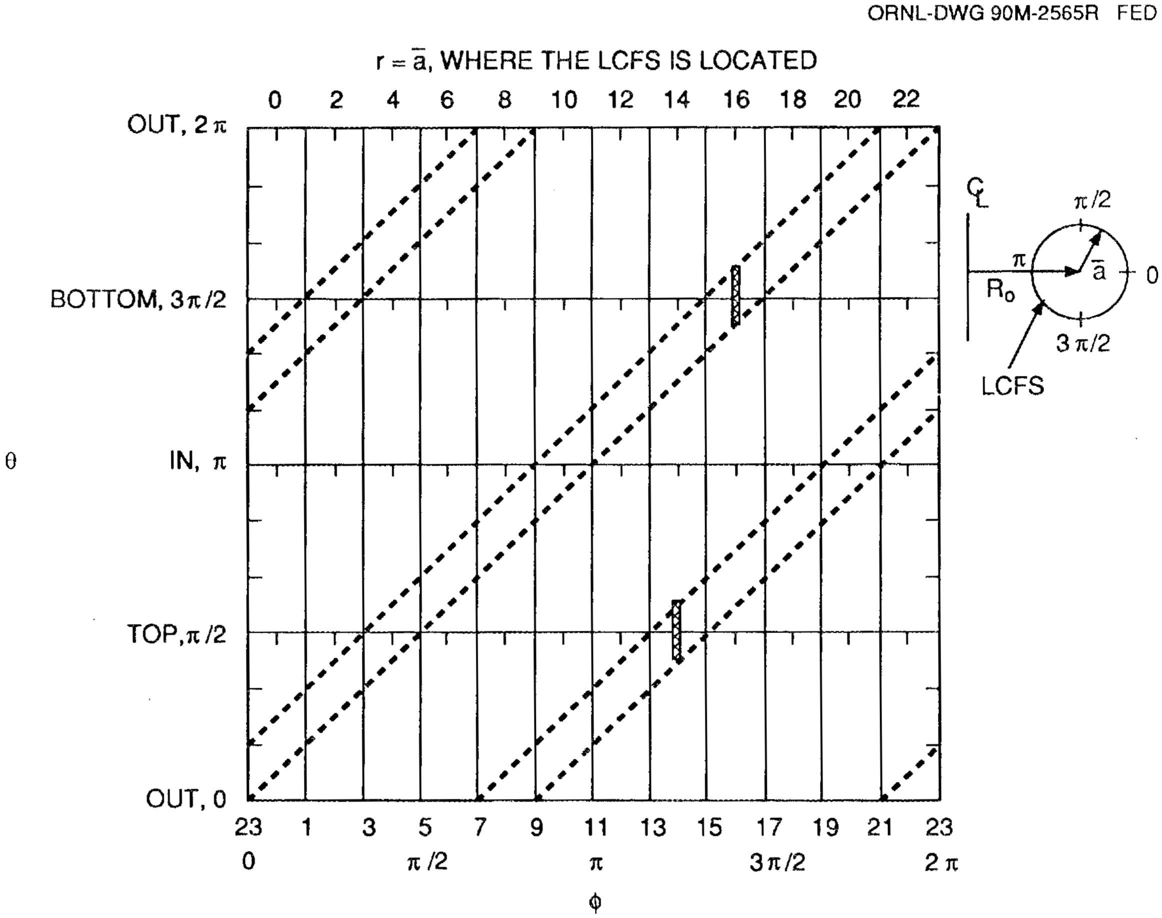

FIG. 8. The location of the top (Port 14) and bottom (Port 16) ATF limiters on the LCFS, $q = 1$, given in terms of a cylindrical geometry in poloidal angle (θ), and toroidal angle (ϕ) space. Each limiter defines a flux tube through which the SOL particles flow and become available for deposition. These two limiters do not shadow each other.

because of the low edge safety factor, $q \sim 1$ rather than $q \sim 3$ as in a typical tokamak, at the natural boundary of the ATF plasma (which results from the magnetic stellarator configuration of this current-free device). The power handling capability of the vessel wall is an important issue because long-pulse (>5-s) operations are planned for ATF. Therefore, this issue will be investigated further both with more experiments and with new diagnostics. For example, the helical field coil troughs inside the vessel wall will be instrumented with thermocouples. Some new sets of instrumented limiters introduced from the inner wall are also planned.

Direct measurement of the total limiter flux Φ_{Lim} is possible in the limiter biasing experiments that will be carried out in the near future. These experiments are expected to provide additional information on the power and particle balance on ATF.

ACKNOWLEDGMENTS

The authors are grateful to J. L. Dunlap for his encouragement and to the members of the ATF group for their cooperation in this work.

REFERENCES

COLCHIN R. J. *et al.* (1990) Phys. Fluids B **2**, 1347.

HAHS C. L. *et al.* (1987) *Proc. 12th IEEE Symp. on Fusion Engineering,* Monterey (Institute of Electrical and Electronics Engineers, New York) p. 243.

HIROE S. *et al.* (1990) Radiation loss measured by bolometer in ATF (unpublished).

LYON J. F. *et al.* (1986) *Fusion Technol.* **10**, 179.

MIODUSZEWSKI P. K. *et al.* (1987) *J. Nucl. Mater.* **145–147**, 210.

MIODUSZEWSKI P. K. *et al.* (1989) *Proc. 16th European Conf. on Controlled Fusion and Plasma Physics,* Venice (European Physical Society, Geneva) Vol. 13B, p. 623.

STANGEBY P. C. (1986) in *Physics of Plasma-Wall Interactions in Controlled Fusion,* POST D. E. and BEHRISCH R., Eds. (Plenum, New York) p. 41.

THOMAS E. W. (1984) in *Data Compendium for Plasma-Surface Interactions* (IAEA, Vienna) p. 98.

UCKAN T. *et al.* (1988a) *Bull. Am. Phys. Soc.* **33**, 2069.

UCKAN T. *et al.* (1988b) *Fusion Technol.* **13**, 165.

UCKAN T. *et al.* (1989) *Bull. Am. Phys. Soc.* **34**, 1947.

ORNL/TM-11520
Dist. Category UC-426

INTERNAL DISTRIBUTION

1. Director, Fusion Energy Division
2. C. C. Baker
3. M. J. Saltmarsh
4. L. A. Berry
5. B. A. Carreras
6. R. A. Dory
7. J. L. Dunlap
8. H. H. Haselton
9. M. S. Lubell
10. T. E. Shannon
11–12. Laboratory Records Department
13. Laboratory Records, ORNL-RC
14–15. Central Research Library
16. Document Reference Section
17. Fusion Energy Division Library
18–19. Engineering Technology/Fusion Energy Division Publications Office
20. ORNL Patent Office
21. R. P. Leinius
22–30. T. Uckan
31. J. D. Bell
32. R. J. Colchin
33. J. H. Harris
34. D. L. Hillis
35. S. Hiroe
36. L. D. Horton
37. R. C. Isler
38. T. C. Jernigan
39. J. F. Lyon
40. P. K. Mioduszewski
41. M. Murakami
42. D. A. Rasmussen
43. J. B. Wilgen
44. W. R. Wing

EXTERNAL DISTRIBUTION

45. Office of the Assistant Manager for Energy Research and Development, U.S. Department of Energy, Oak Ridge Operations Office, P.O. Box E, Oak Ridge, TN 37831
46. D. E. Baldwin, Institute for Fusion Studies, The University of Texas at Austin, RLM 11.222, Austin, TX 78712-1060
47. R. W. Conn, Department of Chemical, Nuclear, and Thermal Engineering, University of California, Los Angeles, CA 90024
48. R. Parker, Plasma Fusion Center, Massachusetts Instiute of Technology, 167 Albany Street, NW16-288, Cambridge, MA 02139
49. K. I. Thomassen, Lawrence Livermore National Laboratory, L-637, P.O. Box 5511, Livermore, CA 94550

50. J. D. Callen, Department of Nuclear Engineering, University of Wisconsin, Madison, WI 53706-1687
51. N. A. Davies, Acting Director, Office of Fusion Energy, Office of Energy Research, ER-50 Germantown, U.S. Department of Energy, Washington, DC 20545
52. S. O. Dean, Fusion Power Associates, Inc., 2 Professional Drive, Suite 248, Gaithersburg, MD 20879
53. H. K. Forsen, Bechtel Group, Inc., Research Engineering, P.O. Box 3965, San Francisco, CA 94119
54. R. W. Gould, Department of Applied Physics, California Institute of Technology, Pasadena, CA 91125
55. R. A. Gross, Plasma Research Laboratory, Columbia University, New York, NY 10027
56. D. M. Meade, Princeton Plasma Physics Laboratory, P.O. Box 451, Princeton, NJ 08543
57. M. Roberts, International Programs, Office of Fusion Energy, Office of Energy Research, ER-52 Germantown, U.S. Department of Energy, Washington, DC 20545
58. W. M. Stacey, School of Nuclear Engineering and Health Physics, Georgia Institute of Technology, Atlanta, GA 30332
59. D. Steiner, Nuclear Engineering Department, NES Building, Tibbetts Avenue, Rensselaer Polytechnic Institute, Troy, NY 12181
60. R. Varma, Physical Research Laboratory, Navrangpura, Ahmedabad 380009, India
61. Bibliothek, Max-Planck Institut für Plasmaphysik, Boltzmannstrasse 2, D-8046 Garching, Federal Republic of Germany
62. Bibliothek, Institut für Plasmaphysik, KFA Jülich GmbH, Postfach 1913, D-5170 Jülich, Federal Republic of Germany
63. Bibliothek, KfK Karlsruhe GmbH, Postfach 3640, D-7500 Karlsruhe 1, Federal Republic of Germany
64. Bibliothèque, Centre de Recherches en Physique des Plasmas, Ecole Polytechnique Fédérale de Lausanne, 21 Avenue des Bains, CH-1007 Lausanne, Switzerland
65. J. Tachon, CEN/Cadarache, Departement de Recherches sur la Fusion Contrôlée, F-13108 Saint-Paul-lez-Durance Cedex, France
66. Bibliothèque, CEN/Cadarache, F-13108 Saint-Paul-lez-Durance Cedex, France
67. Library, AEA Fusion, Culham Laboratory, Abingdon, Oxfordshire, OX14 3DB, England
68. Library, JET Joint Undertaking, Abingdon, Oxfordshire OX14 3EA, England
69. Library, FOM-Instituut voor Plasmafysica, Rijnhuizen, Edisonbaan 14, 3439 MN Nieuwegein, The Netherlands
70. Library, National Institute for Fusion Science, Chikusa-ku, Nagoya 464-01, Japan
71. Library, International Centre for Theoretical Physics, P.O. Box 586, I-34100 Trieste, Italy
72. Library, Centro Richerche Energia Frascati, C.P. 65, I-00044 Frascati (Roma), Italy
73. Library, Plasma Physics Laboratory, Kyoto University, Gokasho, Uji, Kyoto 611, Japan
74. Plasma Research Laboratory, Australian National University, P.O. Box 4, Canberra, A.C.T. 2601, Australia
75. Library, Japan Atomic Energy Research Institute, Naka Fusion Research Establishment, 801-1 Mukoyama, Naka-machi, Naka-gun, Ibaraki-ken, Japan
76. G. A. Eliseev, I. V. Kurchatov Institute of Atomic Energy, P.O. Box 3402, 123182 Moscow, U.S.S.R.
77. V. A. Glukhikh, Scientific-Research Institute of Electro-Physical Apparatus, 188631 Leningrad, U.S.S.R.
78. I. Shpigel, Institute of General Physics, U.S.S.R. Academy of Sciences, Ulitsa Vavilova 38, Moscow, U.S.S.R.
79. D. D. Ryutov, Institute of Nuclear Physics, Siberian Branch of the Academy of Sciences of the U.S.S.R., Sovetskaya St. 5, 630090 Novosibirsk, U.S.S.R.
80. O. Pavlichenko, Kharkov Physical-Technical Institute, Academical St. 1, 310108 Kharkov, U.S.S.R.

81. Deputy Director, Southwestern Institute of Physics, P.O. Box 15, Leshan, Sichuan, China (PRC)
82. Director, The Institute of Plasma Physics, P.O. Box 26, Hefei, Anhui, China (PRC)
83. R. A. Blanken, Experimental Plasma Physics Research Branch, Division of Applied Plasma Physics, Office of Energy Research, ER-542, Germantown, U.S. Department of Energy, Washington, DC 20545
84. R. A. E. Bolton, IREQ Hydro-Quebec Research Institute, 1800 Montée-Ste.-Julie, Varennes, P.Q. JOL 2P0, Canada
85. D. H. Crandall, Experimental Plasma Physics Research Branch, Division of Applied Plasma Physics, Office of Energy Research, ER-542, Germantown, U.S. Department of Energy, Washington, DC 20545
86. R. L. Freeman, General Atomics, P.O. Box 85608, San Diego, CA 92138-5608
87. K. W. Gentle, RLM 11.222, Institute for Fusion Studies, University of Texas, Austin, TX 78712
88. R. J. Goldston, Princeton Plasma Physics Laboratory, P.O. Box 451, Princeton, NJ 08543
89. J. C. Hosea, Princeton Plasma Physics Laboratory, P.O. Box 451, Princeton, NJ 08543
90. D. Markevich, Division of Confinement Systems, Office of Energy Research, ER-55, Germantown, U.S. Department of Energy, Washington, DC 20545
91. R. H. McKnight, Experimental Plasma Physics Research Branch, Division of Applied Plasma Physics, Office of Energy Research, ER-542, Germantown, U.S. Department of Energy, Washington, DC 20545
92. E. Oktay, Division of Confinement Systems, Office of Energy Research, ER-55, Germantown, U.S. Department of Energy, Washington, DC 20545
93. W. L. Sadowski, Fusion Theory and Computer Services Branch, Division of Applied Plasma Physics, Office of Energy Research, ER-541, Germantown, U.S. Department of Energy, Washington, DC 20545
94. J. W. Willis, Division of Confinement Systems, Office of Energy Research, ER-55, Germantown, U.S. Department of Energy, Washington, DC 205
95. A. Perez Navarro, Division de Fusion, CIEMAT, Avenida Complutense 22, E-28040 Madrid, Spain
96. Laboratory for Plasma and Fusion Studies, Department of Nuclear Engineering, Seoul National University, Shinrim-dong, Gwanak-ku, Seoul 151, Korea
97. J. L. Johnson, Plasma Physics Laboratory, Princeton University, P.O. Box 451, Princeton, NJ 08543
98. L. M. Kovrizhnykh, Institute of General Physics, U.S.S.R. Academy of Sciences, Ulitsa Vavilova 38, 117924 Moscow, U.S.S.R.
99. O. Motojima, National Institute for Fusion Science, Chikusa-ku, Nagoya 464-01, Japan
100. S. Okamura, Institute of Plasma Physics, Nagoya University, Chikusa-ku, Nagoya 464, Japan
101. V. D. Shafranov, I. V. Kurchatov Institute of Atomic Energy, P.O. Box 3402, 123182 Moscow, U.S.S.R.
102. J. L. Shohet, Torsatron/Stellarator Laboratory, University of Wisconsin, Madison, WI 53706
103. H. Wobig, Max-Planck Institut für Plasmaphysik, D-8046 Garching, Federal Republic of Germany
104. F. S. B. Anderson, University of Wisconsin, Madison, WI 53706
105. R. F. Gandy, Physics Department, Auburn University, Auburn, AL 36849-3511
106. H. Kaneko, Plasma Physics Laboratory, Kyoto University, Gokasho, Uji, Japan
107. G. H. Neilson, Princeton Plasma Physics Laboratory, P.O. Box 451, Princeton, NJ 08543
108. S. Sudo, Plasma Physics Laboratory, Kyoto University, Gokasho, Uji, Japan
109. C. E. Thomas, Georgia Institute of Technology, Atlanta, GA 30332
110. H. Yamada, National Institute for Fusion Science, Chikusa-ku, Nagoya 464-01, Japan
111. F. W. Perkins, Princeton Plasma Physics Laboratory, P.O. Box 451, Princeton, NJ 08543
112. T. Obiki, Plasma Physics Laboratory, Kyoto University, Gokasho, Uji, Kyoto, Japan

113. A. Iiyoshi, National Institute for Fusion Studies, Chikusa-ku, Nagoya 464-01, Japan
114. A. J. Wootton, Fusion Research Center, University of Texas, Austin, TX 78712
115–167. Given distribution as shown in DOE/OSTI-4500-R75, Magnetic Fusion Energy (Category Distribution UC-426, Experimental Plasma Physics) (53 copies)